MILITARY TECHNICAL COLLEGE

CAIRO - EGYPT

MECHANISMS OF VORTEX FORMATION, SHEDDING AND ATTENUATION

IN THE NEAR-WAKE OF A BLUNT TRAILING EDGE

AHMED H. LOTFY*

ABSTRACT

The unsteady wake from a blunt trailing-edge has been investigated experimentally. Both cases of fully turbulent and laminar boundary layer at separation have been studied. Intensive flow visualization by hydrogen bubble technique, velocity measurements in the near-wake region and pressure measurements along the surface of the trailing-edge reveal several new aspects of this class of flow. A highly organized oscillations occur in the wake region irrespective of the boundary layer at separation whether it is fully turbulent or laminar. A well defined mechanism for vortex formation and shedding process has been introduced by the aid of topological concepts. Subsequently, a new technique is elaborated for attenuation of the coherent vortical structural, by interference of a splitter plate, in the near-wake region. These findings assists the existence of a powerful mechanism of absolute instability in the near-wake region as suggested in previous investigations.

1. INTRODUCTION

Shedding of vortices from a bluff body or a blunt trailing-edge has been a subject of considerable interest over the past century. There are a wide variety of practical configurations that generate organized vortex streets: vanes and blades in hydraulic and turbomachinery; marine propellers; heat exchanger tubes; tall structures; and bridge decks [10]. A detailed knowledge of the near wake flow structure and the loading on the surface of the body is essential if one is to minimize the onset of structural vibration, generation of noise, and alteration of heat transfer rates from the body. Investigations of the flow-induced vibration of, and the vortex formation from, streamlined bodies having blunt trailing-edges has been carried out by [4] and [12]. In the following, attention is focused on selected, critical issues that are to be addressed in the present investigation.

The first class of present issues involves the effects of turbulent, vs. laminar, conditions at separation. One expects, of course, that a well-defined laminar boundary layer at separation will give rise to highly organized oscillations in the near-wake region. However, a point of major interest is whether a fully turbulent boundary layer separation will evolve into a highly coherent near-wake instability.

* Lecturer, Dept. of Mech. Power Eng. & Energy, MTC, Cairo, Egypt.

However, the possible existence of an absolute, as opposed to a convective, instability in the near-wake region may allow self-excited, highly organized vortex formation to emerge from a fully turbulent condition at separation, as explained in ¡6¿. It is well known that large amplitude excitation of convectively unstable mixing layers from thin trailing-edges can produce large-scale coherent structures ¡3¿. If one could observe a similar degree of organization and large-scale structure development in the near-wake region, in absence of excitation of turbulent boundary layers from a thick trailing-edge, then one would have a verification, albeit indirect, of the existence of a strong, self-excited absolute instability of the near-wake. If so, this transformation from a fully turbulent flow to a highly organized one is of fundamental importance in the area of transition and turbulence.

The second class of issues to be addressed concerns means of attenuation of the near-wake vortex formation. The question is; How is it possible to prevent the formation of the large-scale vortices? A better understanding of the mechanism of vortex shedding into the near-wake region would allow determination of the optimum conditions for attenuating the vortex shedding and thereby control the instability of the flow field in the near-wake.

2. EXPERIMENTAL SYSTEM AND INSTRUMENTATION

All experimental investigations were carried out in a large-scale water channel shown in Figure 2.1. The entire channel is made of Plexiglas in order to allow viewing of the flow structure from an arbitrary direction. A special test section insert, which houses the trailing-edge arrangement is located within the main portion of the water channel. This insert has an internal width smaller than the width of the channel in order to allow trimming of the vertical wall boundary layers of the channel and thereby minimization of wall effects. This test section insert also avoids free-surface effects. Details of the experimental arrangement and set up can be found in ¡8¿.

In case of laminar boundary layer at separation, a short plate was designed with an elliptical leading edge having a minor to major axis ratio of 1:5. The total plate length L = 455 mm and thickness T = 25 mm give $Re_L = 2.51 \times 10^4$ and $Re_T = 1400$. To generate a fully turbulent boundary-layer at separation, a long plate was designed with a circular leading-edge and equipped with a boundary-layer trip section, in form of two thin rubber sheets covered with randomly distributed irregularly-shaped plastic-particles. The long plate length L = 1525 mm and thickness T = 25 mm give $Re_L = 3.78 \times 10^5$ and $Re_T = 6.3 \times 10^3$. Continuously variable velocities up to a maximum flow velocity of 0.35 m/sec were attainable in the channel test section.

2.1. Flow Visualization Using Hydrogen Bubble Technique

Visualization of the unsteady flow field was carried out by using hydrogen bubble technique. Two types of hydrogen bubble wires were employed: a straight (undistorted) platinum wire; and a zigzag wire. The conceptual details of the hydrogen bubble technique are described in ¡12¿. The bubble sheet was illuminated by a large-scale stroboscopic light located above the channel at an angle of 30° from the plane of the hydrogen bubble sheet (wire). This stroboscopic light was interfaced to the main frame of the Instar split-screen video system.

The platinum wire was oriented vertically and located a distance of 3 mm downstream of the trailing-edge. The anode for the electrolysis was located exterior to the test section at a distance of 500 mm from the trailing-edge. To complement the foregoing type of visualization, a zigzag wire was employed. The wire was placed vertically at a distance $x/T = 0.75$ downstream of the trailing-edge, where x is the streamwise distance from the edge and T is the trailing-edge thickness. This wire allowed study of vortex formation process in the near-wake region, as will be explained later.

Recording of the flow visualization was carried out with a high speed video recording system, which could be played back in real time or in slow motion in a flicker frame mode. Slow motion playback in the forward direction can be carried out at speeds continuously variable from zero to fifteen percent of real time. The frame-by-frame and stop action capability, as well as the slow motion feature, were used extensively for detailed analysis of the recorded data. Hard copies of the video images were obtained by photographing the video screen in the still-frame mode with a 35 mm camera.

2.2. Pressure And Velocity Measurement Techniques

To provide a quantitative basis for relating the downstream flow structure to the surface pressure field on the edge and the velocity field in near-wake region, measurements were carried out and compared with the results of the flow visualization.

Velocity measurements were carried out using a hot film probe and a traversing mechanism, as illustrated in Figure 2.1. This traversing mechanism allowed computer-controlled movement of the probe to an arbitrary position in the x-y plane by means of a stepping motor arrangement. The signal from the hot-film probe was transmitted to a constant temperature anemometer, then through a linearizer and a voltmeter. Subsequently, this linearized signal was filtered in order to eliminate undesirable and physically meaningless spectral components. The fluctuating pressure was measured using a semiconductor-bonded strain gauge pressure transducer. The pressure transducer was mounted on the extension of the trailing-edge protruding through the false wall shown in the schematic of Figure

2.1. The output from the transducer was fed to a differential amplifier. This amplified pressure signal was fed to a filter as mentioned in the velocity measurements. The output of the amplifiers could be displayed on a storage oscilloscope and their values simultaneously recorded on voltmeters. The signals were then fed to the analog/digital interfaces of a PDP 11/23 minicomputer in order to perform the spectral analysis and correlations.

3. VISUALIZATION OF FLOW STRUCTURE

Extensive flow visualization has been carried out for both cases of laminar and turbulent boundary layer at separation. A comparison between the two flow structures is illustrated in Figure 3.1.

3.1. Laminar Boundary Layer At Separation

In the present study, the flow structure of the near-wake will be the subject of interest, particularly the vortex shedding process according to the separation frequency f_o. The power spectrum, of pressure and velocity signals from the trailing-edge of thickness $T = 25$ mm and at upstream free flow velocity of 0.0575 m/sec, detected the value of the natural vortex shedding frequency $f_o = 0.47$Hz. The corresponding Strohal number is St $= 0.21$.

Figure 3.2a shows the trajectories of vortices shed from the upper and lower corners of the trailing-edge; the successive instantaneous positions of a given vortex are indicated by the black dots. The vortex trajectories were determined by tracking the center of concentration of hydrogen bubbles, corresponding to the position of vortices, on the video screen. The time between successive black dots, representing the successive instantaneous positions of the given vortex, was maintained constant for all cases. This time interval corresponds to 10 frames on the video monitor. A greater distances between successive black dots therefore represents a higher value of velocity. It is evident that after the vortex reaches its location closest to the centerline of the flow, there is an abrupt increase in velocity as it *departs* and moves outward away from the centerline. The vortex formation length L_F is defined here to occur when the position of the vortex is closest to the centerline of the flow.

The trajectories of Figure 3.2a can be plotted in the form of streamwise displacement x_v of the vortex vs. time t, as illustrated in Figure 3.2b and the cross-stream displacement y_v vs. time t, as illustrated in Figure 3.2c. Considering first the trajectory x_v vs. of Figure 3.2b, there are several general observations to be made. The initial portion of the trajectory for $x/T < 0.4$ has a relatively considerable lower slope than the trajectory at the other extreme well downstream of the trailing-edge, for $x/T > 2.4$. This behavior suggests the existence of two different phases for the shedding process of vortices into the near wake region. A careful study, of

the recorded tape, for the flow structure in the near-wake region, showed that the first process was the *formation* of vortex by ingestion of the separating fluid from one side of the plate into the near-wake region ($x/T < 0.4$), where dx_v / dt is considerably slow. The second process was its *departure* by the effect of the ingested fluid from the opposite side of the plate where the conjugate vortex was being formed. Therefore, the entrained fluid departs the formed vortex at a higher rate of dx_v / dt into the near-wake region ($x/T > 2.4$).

Similar considerations hold for the trajectory y_v vs. t of Figure 3.2c. Calculation of the slope of the trajectory y_v vs. t, at a reference location $x/T = 0.1$, showed that the vertical velocity dy_v / dt has a negative vertical velocity towards the centerline of the flow during *formation* process of the vortex, and a positive vertical velocity away from the centerline during its *departure* process. The vertical velocity dy_v / dt of the vortex is zero, when the center of the vortex is nearly at midway of edge thickness. This can be explained as follows; in accordance with the analysis of Figure 3.2a, the process of vortex formation is completed and its departure process is initiated when the center of the vortex reaches the closest position to the centerline of the flow.

3.2 Topology Of The Near-Wake Flow Structure

In most experimental investigations of unsteady flows, the instantaneous streamline patterns are usually ignored in favor of streakline visualization. Of course, in an unsteady flow, the relationship between instantaneous streamlines and streaklines is not obvious and without full knowledge of the velocity field, it is not possible to determine the exact relationship between them. However, it can be shown that over very short time intervals, streaklines, pathlines and instantaneous streamlines are identical, e.g. ¡7¿.

The main objective of the present investigation is to carry out extensive flow visualization using streakline and timeline methods to obtain selected instantaneous streamline patterns in the near-wake of the body. By using this combined approach, it is anticipated that new insight can be gained into the unsteady flow structure. These patterns will provide insight into the entrainment process in the near-wake region in conjunction with critical-point concepts. Concurrently, the mechanism of vortex formation in the near-wake region will be studied by interpreting the flow visualization

To provide a quantitative basis for construction of the near-wake topology, tracking of hydrogen bubble elements was carried out. The hydrogen bubbles were generated using the zigzag hydrogen bubble wire. These bubble elements were located on the screen at certain phase of vortex shedding process. The location of all bubble elements were recorded on a transparency at this position of the edge. The video film was advanced forward by $20°$ and the new location of all bubble elements were recorded on the transparency, then the displacement

position of each bubble was marked. In this manner, it was possible to determine the displacement of each bubble element over the defined time interval, and thereby obtain a representation of the instantaneous velocity field as shown in Figure 3.3a. Instantaneous streamlines were approximated by considering the local tangents to the velocity vectors. Figure 3.3b shows the approximated streamline patterns, as well as symbols indicating key topological definitions.

3.3. Phase clock of near-wake from stationary edge

Figure 3.4a. shows the definition of the terminology used for constructing the so called a phase clock, to explain the mechanism of vortex shedding process as observed on the video screen. Figure 3.4b shows one complete cycle of vortex shedding process. The specific instant or *phase* corresponding to the onset of vortex formation from the upper surface of the edge is arbitrarily placed at 6:00. At the phase corresponding to 12:00, the formation of the vortex from the upper surface of the edge is completed and there is onset of vortex formation from the lower surface. At the phase corresponding to 6:00, formation of vortex from the lower side is completed and there is onset of a new vortex formation process from the upper side. With regard to departure of the upper and lower vortices, the departure process of each vortex begins when its formation ends.

In summary, for vortex shedding from the trailing-edge, we have the remarkable result that all of the vortex formation and departure times have the same value and are equal to the half period $0.5T_o$ of vortex shedding from the stationary edge, i.e. $0.5T_o = T_{FU} = T_{FL} = T_{DU} = T_{DL}$. In physical sense, the onset of formation of a given vortex and the completion of vortex departure of its predecessor (of the same circulation) occur at the instant when there is onset of ingestion of boundary-layer fluid (past the corner) into the incipient vortex.

3.4. Effect Of Turbulent Initial Conditions On Flow Structure

The question arises as to whether the basic characteristics of the flow structure and surface pressure loading described in section 3.1 can exist in presence of a fully turbulent boundary layer at separation? The basic hypothesis is that the instability in the near-wake is predominantly due to inviscid mechanisms. If there exists an absolute instability in the near-wake [9], then it is possible that the self-excitation mechanism associated with this absolute instability can override the random effects of the turbulent boundary layer separating from the trailing-edge.

Visualization of near-wake vortex formation, in case of stationary trailing-edge, is shown in Figure 3.1. It is obvious that there exists a very well coherent vortex structural in the near wake region, in presence of turbulent flow, which prove the existence of absolute

instability as discussed before. The question now is whether we can attenuate this vortical structure or not? From the present findings of the vortex shedding mechanism, it is possible to attenuate this vortical structure if we could stop the vortex formation process. Eventually, the attenuation process was realized by placing a splitter plate, in a critical position, downstream of the trailing-edge. This position was in the alleyway of the entrained fluid which departs the formed vortex. It means that, when the departure process of a formed vortex was prevented or obstructed then the production of more vortices could be stopped. In the following section more details of the method of vortex attenuation are given.

4. ATTENUATION OF COHERENT VORTEX STRUCTURE IN NEAR-WAKE

The fact that the near-wake oscillation can be attenuated with small interference is indicated in Figures 4.1 through 4.3. A brass plate (blade), having a thickness of 3 mm and a width of 12.5 mm spanning the entire test section, was placed such that its axis of symmetry was at a location $x/T = 1.6$ downstream of the trailing-edge. Deployment of the blade at this location effectively attenuates the large-scale vortex shedding process.

4.1 Autocorrelation Measurements Of Pressure And Velocity

In addition to visualization, a quantitative measurement technique were employed in order to give proof of attenuation process. The autocorrelation measurement, of detected pressure and velocity signals, were carried out for both cases of near-wake flow structures with and without placing the attenuation plate in the critical position.

The autocorrelation function $R_x(\tau)$ is defined as,

$$R_x(\tau) = E(x(t)x(t+\tau)) = 1/T \left(\int_0^T x(t)x(t+\tau) \, d\tau \right)$$

in which T is the sampling time period.
* The autocorrelation
coefficient $\rho(\tau)$ is defined as the ratio of the autocorrelation function $R_x(\tau)$ to the variance σ^2 when the zero value of the random process $x(t)$ is normalized so that the mean value of the process $x(t)$ is zero. It takes the form:

$$\rho(\tau) = R_x(\tau) / \sigma^2$$

The autocorrelation coefficient given above was calculated for the pressure signal detected at the trailing-edge, as well as for velocity signals along the edge of the shear-layer. Figure 4.2 shows the autocorrelation of the pressure signal on the vertical surface of the trailing-edge at location $(x/T = 0, y/T = 0.4)$. Figure 4.3 shows the autocorrelation of the velocity signal where the hot film probe is placed at $x/T = 2.8$ along the edge of the shear-layer downstream the trailing-edge.

Examination of the autocorrelation for the pressure signal shows the
following trends. Figure 4.2a shows the autocorrelation coefficient
of the pressure signal at (x/T = 0, y/T = 0.4) *without* the attenuation
blade in attenuation position. It represents a highly organized
oscillation in the near-wake region. This observation is remarkable
in view of the fact that the boundary-layer at separation is fully
turbulent. Figure 4.2b shows the autocorrelation coefficient of the
pressure signal at x/T = 0 *with* the attenuation blade in its effective
position, x/T = 1.6 downstream the trailing-edge. The autocorrelation
has a form reminiscent of a turbulent flow (stationary random
process).

For the autocorrelations of the velocity signal, the following trends
are evident. Figure 4.3a shows representative variations of the
autocorrelation coefficient of the velocity signal *without* the blade
in the attenuation position. It represents a quasi-organized process
as does the pressure signal, due to existence of the organized
vortical structures. Autocorrelations at other probe locations along
the edge of the shear-layer showed similar behavior. Figure 4.3b
shows the autocorrelation coefficient for the velocity signal *with* the
blade in the attenuation position (at x/T = 1.6). It represents a
stationary random process, evidenced by lack of organized vortical
structure in the flow visualization.

5. OVERVIEW AND CONCLUSIONS

* The wake from a stationary, bluff trailing-edge can exhibit a highly
organized, self-excited instability. This type of instability,
which has been recently characterized theoretically in terms of
absolute instability concepts [9], shows a high degree of coherence,
even in presence of a fully turbulent boundary layer at separation.
One may view this self-excited instability as a nonlinear
oscillator.

* The effect of a turbulent boundary layer separating from the
trailing-edge has been examined, relative to the case of the laminar
boundary layer employed in the foregoing. In essence, all of the
principal features of the unsteady and time-averaged near-wake, as
described in the preceding, occur in the presence of a fully
turbulent boundary layer at separation. This observation
underscores the power of the absolute instability in the near-wake
region: a fully turbulent flow rapidly evolves into one exhibiting
highly organized vortical structures. From a theoretical
standpoint, since the absolute instability analysis is an inviscid
one, one may view the effect of turbulence as simply changing the
time-mean velocity profile that is perturbed during the absolute
instability.

* The vortical structure is produced by a continuous building up and departure of vortices from the body. Each vortex is formed by the fluid of the separated boundary layer at the vortex side and departed by the effect of the separated flow at the opposite side of the body. The formation process of one vortex overlaps the departure process of the opposite vortex. For stationary edge, the time of formation of a vortex is equal to its time of departure. It means that the vortex shedding frequency is the reciprocal of double of its formation time. In other words, the period of vortex shedding is double of its formation time.

* The highly organized near-wake flow structure in presence of a turbulent boundary layer at separation can be attenuated effectively by stopping the formation operation of the vortices in the near-wake region. This was realized by deploying a small blade in a critical position in the near-wake region. In this case, autocorrelations of the fluctuating surface pressure and the near-wake velocity fluctuations showed a form typical of a fully turbulent flow, in contrast with the case of the non-attenuated wake, where they exhibit a form representative of a quasi-periodic process.

* The effect of trailing edge excitation, with different amplitudes and frequencies, on the flow structure in the near-wake region will be introduced in future work.

6. REFERENCES

1) Blake, W. K. 1984 "Trailing edge flow and aerodynamic sound, Part 1: Tonal pressure and velocity fluctuations; Part 2: Random pressure and velocity fluctuations", Ship Acoustics Department, Research and Development Report, David W. Taylor Naval Ship, Research and Development Center, Bathesda, Maryland, 20084-5000.

2) Blevins, R. D. 1977 "Flow Induced Vibration", Van Nostrand Reinhold Co., London.

3) Fiedler, H. E. and Mensing, P. 1985 "The Plane turbulent shear layer with periodic excitation", J. Fluid Mechanics, vol.150, pp.281-309.

4) Greenway, M. E. and Wood, C. J. 1973 "The effect of bevelled trailing-edge on vortex shedding and vibration", J. Fluid Mechanics, vol. 61, pt. 2, pp. 323-335.

5) Hinze, J. O. 1959 "Turbulence", McGraw-Hill, New York.

6) Huerre, P. and Monkewitz, P. A. 1985 "Absolute and convective instabilities in free shear layers", J. Fluid Mechanics, vol. 159, pp. 151-168.

7) Kline, S.J. 1965 FM-48 Film loop, National Committee for Fluid Mechanics Films.

8) Lotfy, A.H. 1988 "Flow structure and loading due to instability from an oscillating-edge of finite thickness", Ph.D. Dissertation, Mechanical Eng. Dept., Lehigh University, USA, U.M.I. Dissertation Information Service.

9) Monkewitz, P. A. and Nguyen, L. N. 1987 "Absolute instability in the near-wake of two-dimensional bluff bodies", J. Fluids and Structures, vol. 1, pp. 165-187.

10) Naudascher, E. and Rockwell, D. 1980 "Practical experiences with flow-induced vibrations", Springer-Verlag, Berlin.

11) Schlichting, H. 1979 "Boundary Layer Theory", 7th edn., McGraw-Hill, New York.

12) Schraub, F. A., Kline, S. J., Henry, J., Runstadler, P. W., and Little, T. J., 1965 "Use of hydrogen bubbles for qualitative determination of time dependent velocity fields in low-speed water flows", ASME Transactions, J. Basic Engineering, vol.87, pp.429-444.

13) Wood, C. J. 1971 "The effect of lateral vibrations on vortex shedding from blunt based aerofoils", J. Sound and Vibrations, vol. 14, P. 91.
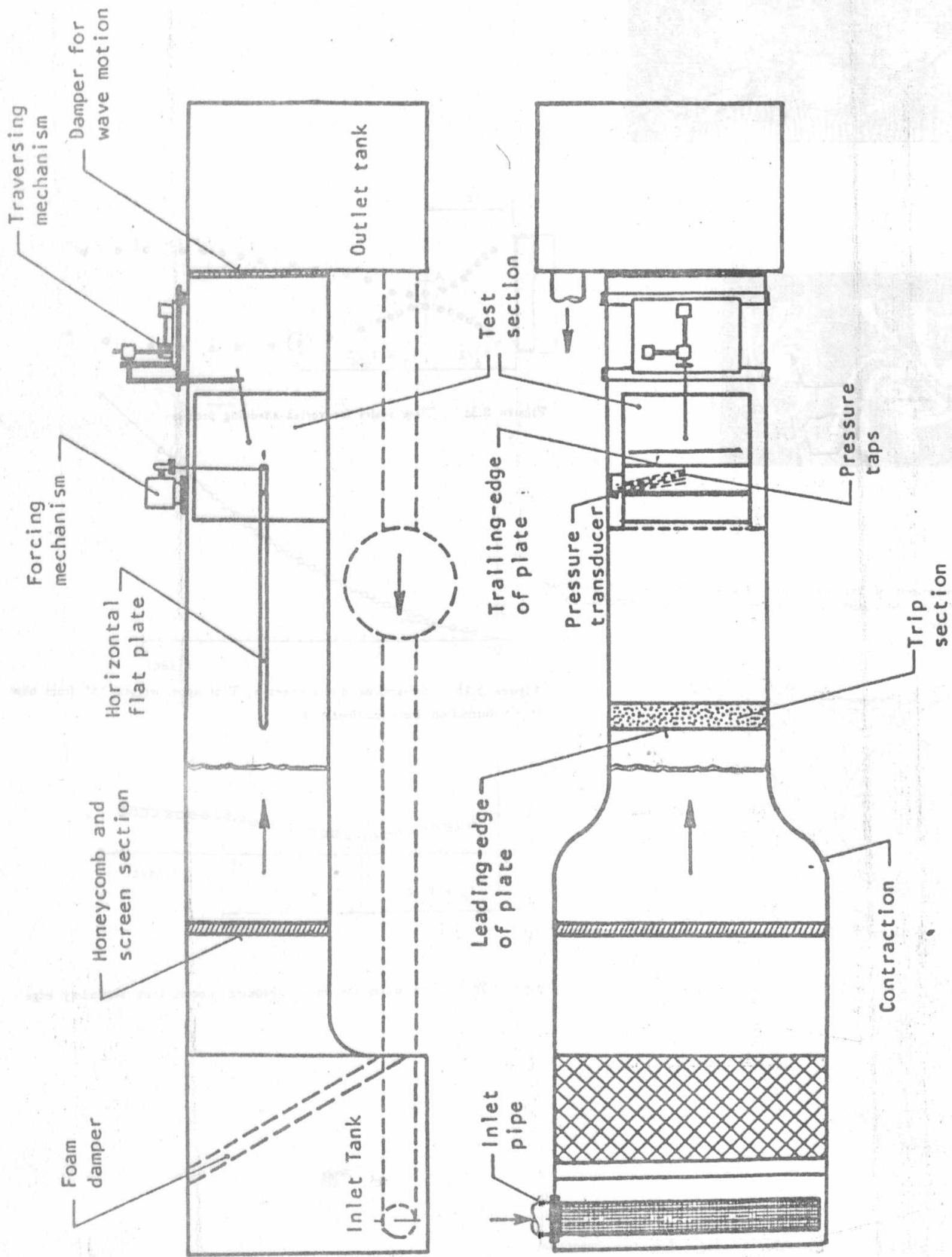
Figure 2.1 : Schematic of water channel system including test section, forcing mechanism, hot film probe holder, and traversing mechanism.

(a)

(b)
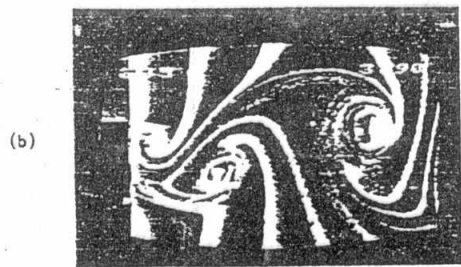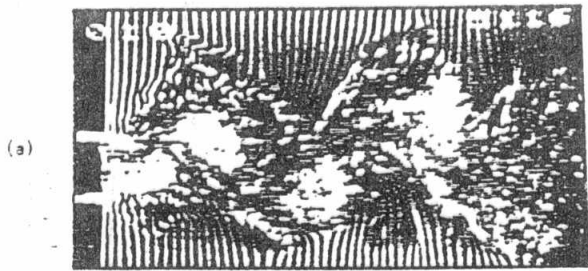
Figure 3.1: Comparison of the visualized vortical flow structure in wake region (a) turbulent (b) laminar boundary layer at separation. Trailing-edge is stationary.
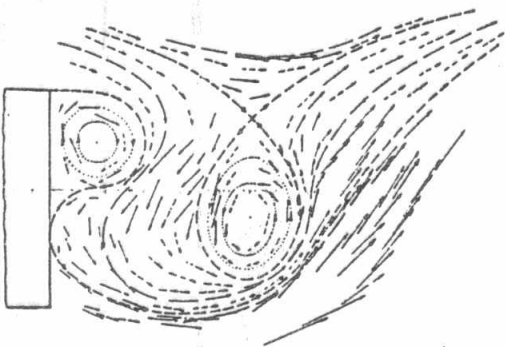

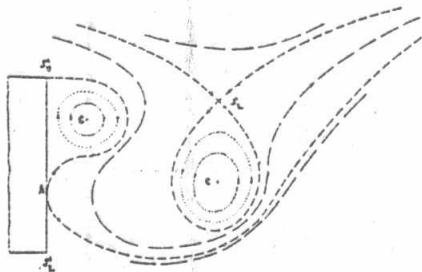Figure 3.2 a: Representation of fields of instantaneous velocity vectors , in

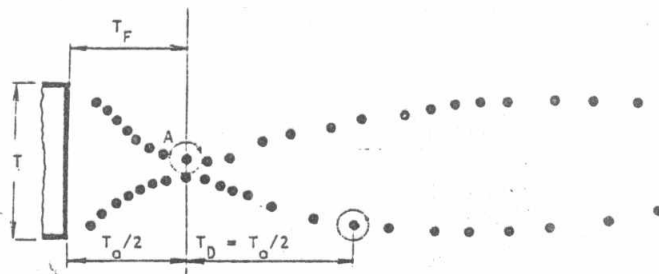Figure 3.2b: Comparison of near-wake topology for two-dimensional interpretations

Figure 3.3a : Time scales for vortex shedding process
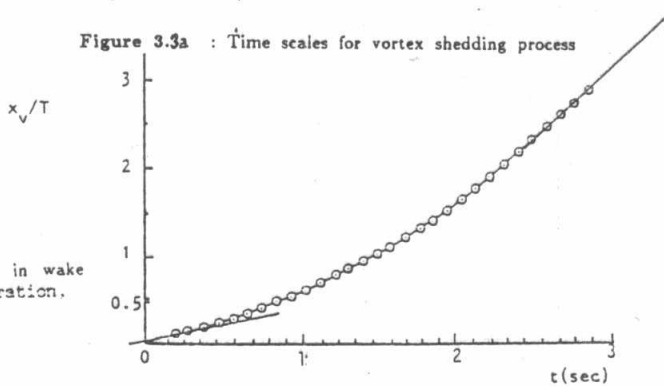
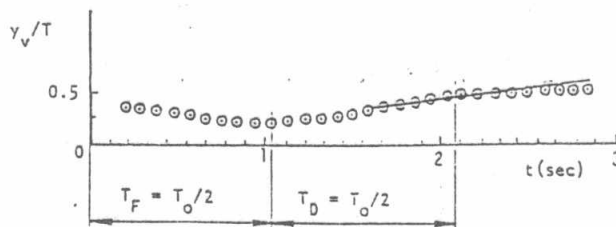Figure 3.3b : Streamwise displacement x_v/T of upper vortex "A" from onse of its formation from stationary edge

Figure 3.3c : Time scales for vortex shedding process from stationary edge
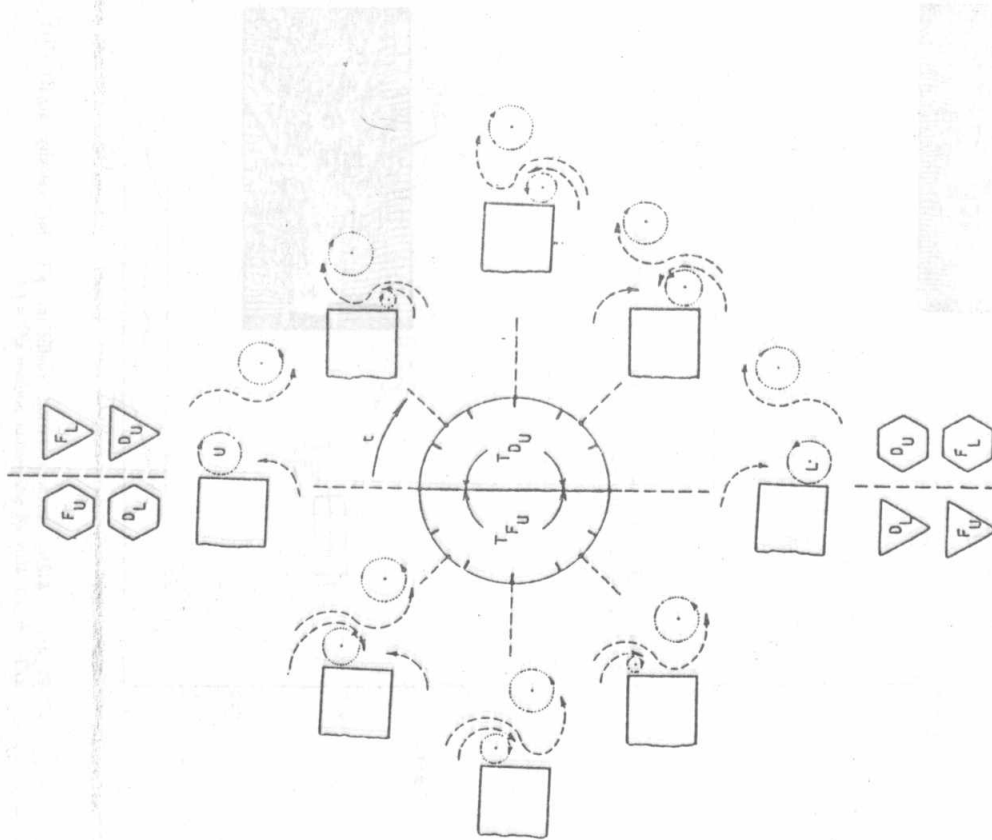
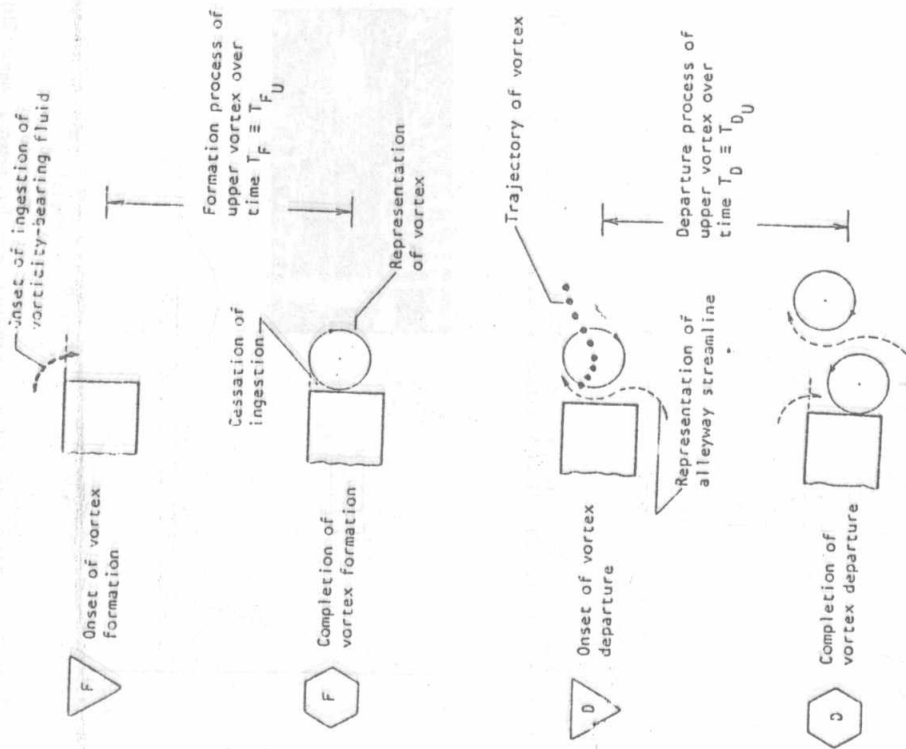Figure 3.4b : Phase clock representation of vortex shedding process at $f_o/f_o^* = 0$.

Onset of vortex formation

Completion of vortex formation

Onset of vortex departure

Completion of vortex departure

Onset of ingestion of vorticity-bearing fluid

Formation process of upper vortex over time $T_F \equiv T_{F_U}$

Representation of vortex

Cessation of ingestion

Trajectory of vortex

Departure process of upper vortex over time $T_D \equiv T_{D_U}$

Representation of alleyway streamline

Figure 3.4a : Definition of terminology for phase clocks.

AD-3 40

Figure 4.2a: Autocorrelation coefficient $\rho(\tau)$ for velocity signal $\tilde{u}(t)$ at $x/T = 3$ without attenuation blade.

Figure 4.2b: Autocorrelation coefficient $\rho(\tau)$ for velocity signal $\tilde{u}(t)$ at $x/T = 3$ with blade at attenuation position $z/T = 1.d$.
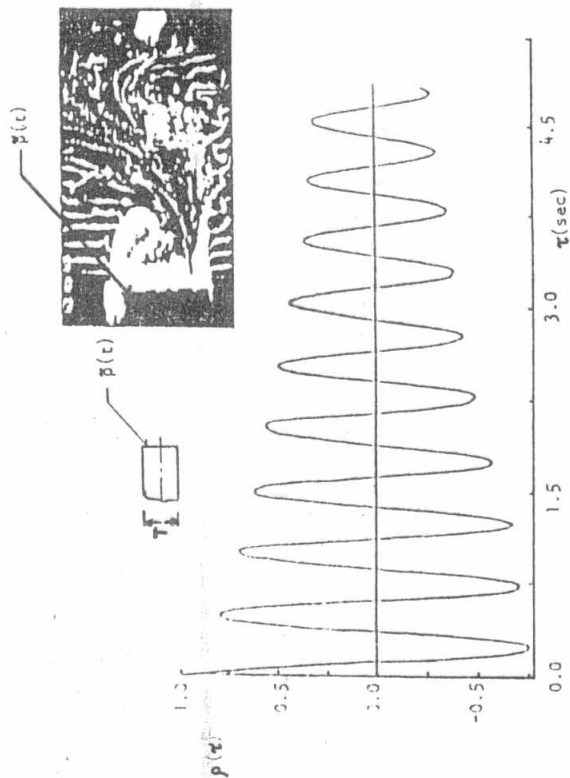
Figure 4.1a: Autocorrelation coefficient $\rho(\tau)$ for pressure signal $\tilde{p}(t)$ at location ($x/T = 0$, $y/T = 0.5$) without attenuation blade.
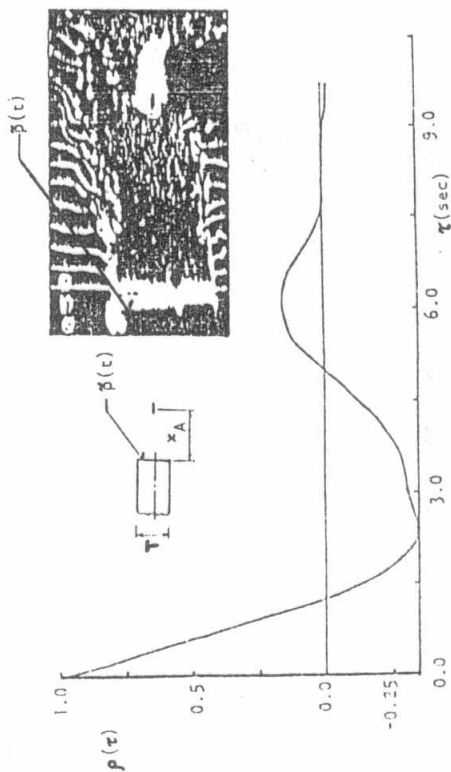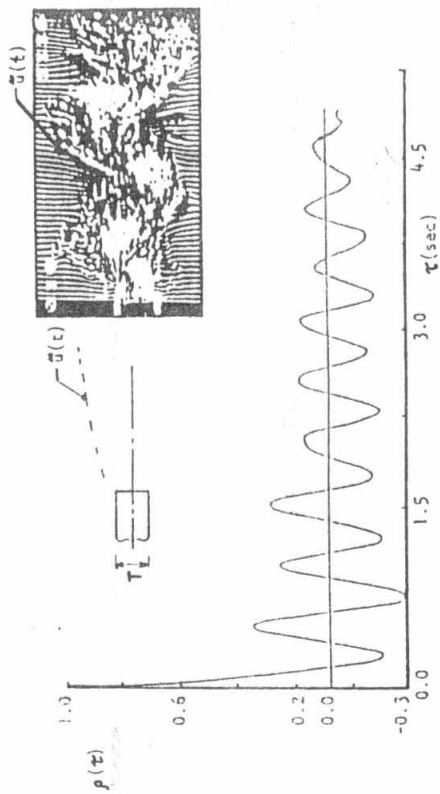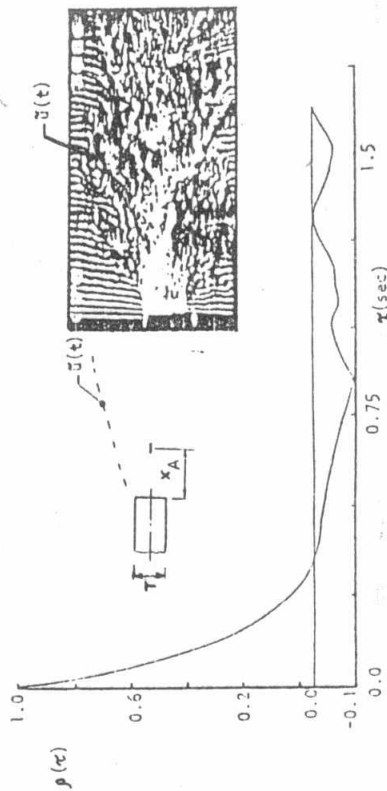

Figure 4.1b: Autocorrelation coefficient $\rho(\tau)$ for pressure signal $\tilde{p}(t)$ at location ($x/T = 0$, $y/T = 0.5$) with blade at attenuation position $x/T = 1.6$.